Letter

Simultaneous Suppression of π- and σ-Transmission in π-Conjugated Molecules

Marc H. Garner and Gemma C. Solomon*

Cite This: *J. Phys. Chem. Lett.* 2020, 11, 7400−7406

Read Online

ACCESS | 📊 Metrics & More | 📰 Article Recommendations | 🆂🅸 Supporting Information

ABSTRACT: Molecular dielectric materials require ostensibly conflicting requirements of high polarizability and low conductivity. As previous efforts toward molecular insulators focused on saturated molecules, it remains an open question whether π- and σ-transport can be simultaneously suppressed in conjugated systems. Here, we demonstrate that there are conjugated molecules where the σ-transmission is suppressed by destructive σ-interference, while the π-transmission can be suppressed by a localized disruption of conjugation. Using density functional theory, we study the Landauer transmission and ballistic current density, which allow us to determine how the transmission is affected by various structural changes in the molecule. We find that in para-linked oligophenyl rings the σ-transmission can be suppressed by changing the remaining hydrogens to methyl groups due to the inherent *gauche*-like structure of the carbon backbone within a benzene ring, similar to what was previously seen in saturated systems. At the same time, the methyl groups fulfill a dual purpose as they modulate the twist angle between neighboring phenyl rings. When neighboring rings are orthogonal to each other, the transmission through both π- and σ-systems is effectively suppressed. Alternatively, breaking conjugation in a single phenyl ring by saturating two carbons atoms with two methyl substituents on each carbon, results in suppressed π- and σ-transport independent of dihedral angle. These two strategies demonstrate that methyl-substituted oligophenyls are promising candidates for the development of molecular dielectric materials.
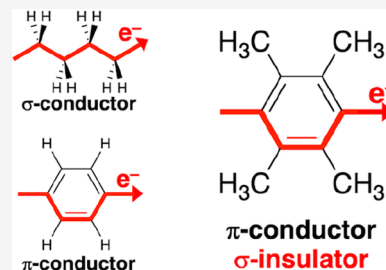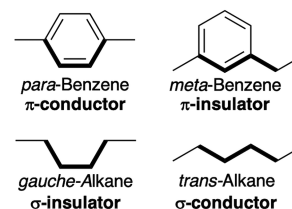
The capacitance of dielectric materials used in the semiconductor industry continues to be limited by leakage currents due to direct tunneling, and by the polarizability of the material.[1−4] This problem means that there is ongoing interest in molecules with extremely low conductance and high polarizability as researchers explore the possibility of molecular dielectric materials.[5−10] However, in a hydrocarbon backbone, π-systems provide the highest polarizability, while saturated molecules have hitherto been found to be the best insulators.[11−14]

While the concept of a conjugated insulator sounds at first to be oxymoronic, there have been hints in this direction. In the low-bias regime, the single-molecule conductance is mediated by a coherent tunneling mechanism that can be suppressed by destructive quantum interference in either the π- or σ-systems.[14−17] Consequently, the conductance of a meta-linked benzene is expected to be much lower than that of *para*- and *ortho*-linked benzenes.[18−22] However, destructive quantum interference has not been predicted or observed to occur in both the π- and σ-systems of a single molecule. For example, only the π-transmission is suppressed in *meta*-benzenes and similar cross-conjugated motifs; thus, Kiguchi et al. found the conductance of *meta*-linked benzenedithiol and benzenediamine to "only" be around half that of their para-linked counterparts as significant σ-transport remains.[23] In general, molecules with π-interference do not achieve lower conductance than alkanes of equivalent length because the σ-transmission is not suppressed.[14,24−27] The conductance

difference between *meta*- and *para*-linked benzenes is therefore larger in longer molecules when σ-transport is naturally suppressed due to faster decay with length.[28−38] An optimal insulating/dielectric molecule will, however, deliver the lowest possible conductance with the shortest possible length. We consider the *para*-case the archetypical π-conductor and the *meta*-case the archetypical π-insulator, as shown in Scheme 1.

We and others recently uncovered chemical design rules for suppression of the σ-transmission in saturated molecules by destructive quantum interference.[14,39−41] The σ-interference
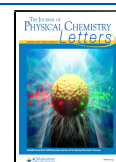
Scheme 1. Transport Properties of Organic Molecular Wires

para-Benzene
π-conductor

meta-Benzene
π-insulator

gauche-Alkane
σ-insulator

trans-Alkane
σ-conductor

effect can appear when there is a gauche defect in the molecular backbone, i.e., a dihedral angle of approximately 60° or less. Furthermore, the suppression is strongest in methyl-substituted species (as opposed to all substituents being hydrogen).[41] Therefore, the interference effect is clearest in the single-molecule conductance of saturated silanes that are generally permethylated, though it is also significant in alkanes.[41−45] By considering *trans*-alkanes the archetypical σ-conductor and *gauche*-alkanes the archetypical σ-insulator, we deduce from Scheme 1 that the structural requirements for π- and σ-interference appear to be mutually exclusive. The σ-path through *meta*-benzene is structurally akin to that of the *trans*-alkane, and the σ-path of *para*-benzene is structurally akin to that of the *gauche*-alkane. It is with this structural analogy in mind that we shall explore if both the π- and σ-transmission of conjugated molecules can be suppressed in a single system.

In this Letter, we explore how both the σ- and π-transmission can be switched off in π-conjugated biphenyl- and triphenyl-based molecules using a combination of structural modifications that both disrupt π-conjugation and support σ-interference. These systems are well-studied both theoretically and experimentally in the context of molecular electronics and are ideal for exploring the σ-transmission in π-conjugated systems because the π-transmission can be controlled by the torsion angle of the phenyl rings.[46−50] The torsion angle can be controlled by the choice of substituents on the phenyl rings, and several molecular systems covering the full range of angles from coplanar to perpendicular orientation have been synthesized.[47−55] This includes methylating the rings, the same substituent pattern that supports maximal destructive σ-interference in saturated molecules.[47−55] When two phenyl rings are orthogonal relative to each other, the π−π coupling will be almost fully suppressed. This alters the electronic properties because π−σ and σ−σ electronic couplings become more important than the π−π coupling,[46,56] e.g., the surprisingly high hyperpolarizability of twisted chromophores.[57−59]

We compute the Landauer transmission and ballistic current density using our in-house transport code, which utilizes the Atomic Simulation Environment (ASE) and GPAW.[60,61] Our code is available as freeware on https://github.com/marchgarner/Current_Density. The methods are described in detail in recent work and in Supporting Information part A.[62,63] Briefly, all molecules are optimized using density functional theory (DFT) with the PBE functional and 6-311G(d,p) basis set as implemented in Gaussian09.[64,65] The optimized structures are rotated without further optimization; thus all degrees of freedom are frozen except for the dihedral angle(s). The transmission and ballistic current density are calculated using DFT in combination with the nonequilibrium Green's functions approach using s-band approximated electrodes. The ballistic current density is calculated in the low-bias limit using a bias of 1 mV, which is opened symmetrically around the Fermi energy. Junction structures are included in xyz format as Supporting Information.

First, we take a simple biphenyl system with and without methyl substituents, as shown in Figure 1a. In agreement with previous work, the transmission at the Fermi energy follows a cosine-squared dependence with the dihedral angle between the phenyl rings. Shown in Figure 1b, the difference between **BPh-H** and **BPh-Me** is negligible on a log scale. In both systems the transmission drops rapidly as the dihedral angles approach 90°. While the methyl substituents are undoubtedly
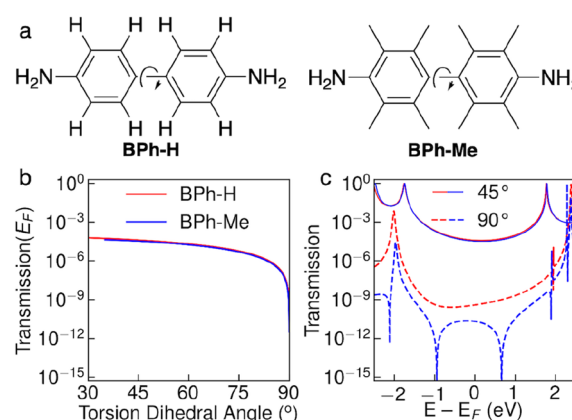

Figure 1. Transmission of biphenyl under axial torsion. (a) Chemical structure of nonmethylated (**BPh-H**) and permethylated (**BPh-Me**) biphenyl functionalized with amine groups. (b) Transmission of **BPh-H** (red) and **BPh-Me** (blue) at the Fermi energy as a function of dihedral angle. (c) Transmission as a function of energy for **BPh-H** (red) and **BPh-Me** (blue) calculated at 45° (full lines) and 90° (dashed lines) dihedral angles.

electron donating compared with hydrogen, this effect does not have a significant impact on the transmission at the Fermi energy. This is also the case if we look at the full transmission plots at 45° in Figure 1c; only small differences are evident and these are not near the Fermi energy. However, at 90° the transmission plots are remarkably different across a large energy range. Both **BPh-H** and **BPh-Me** have low transmission, but in the methylated case two sharp antiresonances appear close to the Fermi energy; a clear signature of suppression due to destructive quantum interference.

At 90° torsion the phenyl rings are orthogonal, and the π−π coupling between the phenyl rings is negligible. Instead, the transmission is mediated by π−σ coupling, i.e., π through one ring and σ through the second (or vice versa). This can be deduced from the current density plots in Supporting Information part B and is in agreement with previous theoretical studies of biphenyl systems.[46,56] As the transmission is mediated in the σ-system in one ring that contains a gauche-like dihedral angle of 0°, the transmission is very low. However, the introduction of methyl substituents in **BPh-Me** induces destructive σ-interference further reducing the transmission compared with **BPh-H**. This behavior upon substitution is similar to what we have recently demonstrated in cyclic and bicyclic silanes and alkanes.[14,41] The appearance of two antiresonances near the Fermi energy is predicted by the Hückel-type Ladder C model (see Supporting Information part C) but is usually not seen in DFT calculations.[39,66,67] We note here that crystal structures obtained on similar biphenyl molecules found the dihedral angles for the hydrogen substituted system to be 36.4° while the methylated system was 89°.[48] The optimized dihedral angles of **BPh-H** and **BPh-Me** are in good agreement with these values, and the transmissions of the optimized structures are included in Figure S9. Thus, while the geometry we find to maximally suppress σ- and π-transmission represents a higher energy structure for **BPh-H**, it is very close to the minimum energy structure for **BPh-Me**.

The suppression of the σ-transmission is even clearer in the triphenyl systems, **TPh-H** and **TPh-Me**, shown in Figure 2a, where a significant reduction in the transmission at the Fermi energy is evident across a wider range of dihedral angles. We
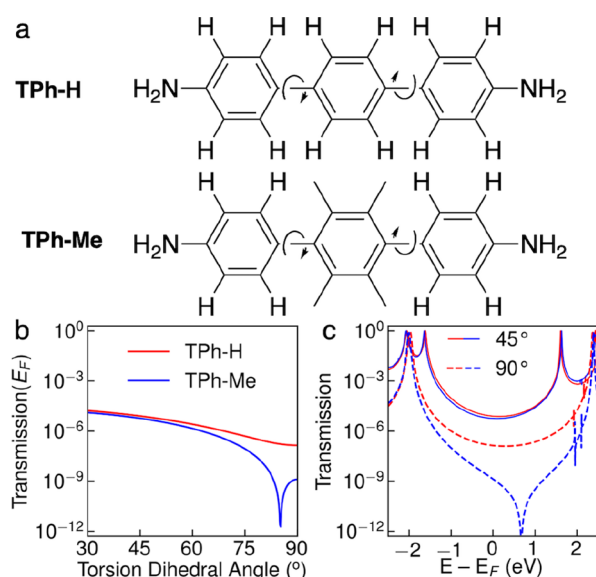
Figure 2. Transmission of triphenyl under axial torsion. (a) Chemical structure of amine-functionalized triphenyl (**TPh-H**) and centrally methylated (**TPh-Me**) triphenyl. (b) Transmission of **TPh-H** (red) and **TPh-Me** (blue) at the Fermi energy as a function of dihedral angle. (c) Transmission as a function of energy for **TPh-H** (red) and **TPh-Me** (blue) calculated at 45° (full lines) and 90° (dashed lines) dihedral angles.

simultaneously rotate the two outer rings relative to the central ring. Only the central ring is methylated in **TPh-Me**. This may shift the minimum energy structure to a lower dihedral angle, and a related biphenyl system with a single methyl substituent on each ring was found from a crystal structure to have a dihedral angle of 79.7°.[48] However, at the level of theory applied in this letter, we find the optimized dihedral angles of **TPh-Me** to be 90.0°, and the transmission plots for the

optimized conformations of **TPh-Me** and **TPh-H** are shown in Figure S9. Shown in Figure 2b, the transmission at the Fermi energy is similar at first but the transmission rapidly drops off in the methylated case as the dihedral angle approaches 90°. The transmission plots in Figure 2c reveal that at 90° the transmission of **TPh-Me** is suppressed in a broad energy range due to an antiresonance near the Fermi energy. The introduction of the otherwise benign methyl substituents on the central ring changes the transmission by several orders of magnitude because of the σ-interference effect. In good agreement with this result, Chen et al. recently reported the single-molecule conductance of a similar methyl-substituted triphenyl system to be surprisingly low.[54]

Let us take a closer look at the interactions that mediate the current in **TPh-H** and **TPh-Me** and in particular the role of the σ and π systems in mediating the current. In a molecule where the π-system dominates the current (oligo-phenyl systems with coplanar rings), we expect to see current density above and below the plane of the benzene rings. On the other hand, if the σ-system is carrying the current, we expect to see current density in the plane of the benzene ring directly through the σ-bonds. These expectations follow the symmetry of the σ and π systems. In Figures 3 and 4, the current density is plotted through two select surfaces of **TPh-H** and **TPh-Me** in the transport direction. To provide navigation, the atoms near each cross-section are shown in the current density heat-maps as colored circles following the designations in Figures 3a and 4a. In Figures 3b and 4b (the first row of current density plots), the surface is chosen through the inter-ring carbon−carbon bond to provide information about the interactions that govern the coupling between the rings. In Figures 3c and 4c (the second row of current density plots), the surface is chosen through the central phenyl ring to provide information about the interactions that govern the transport through this ring.
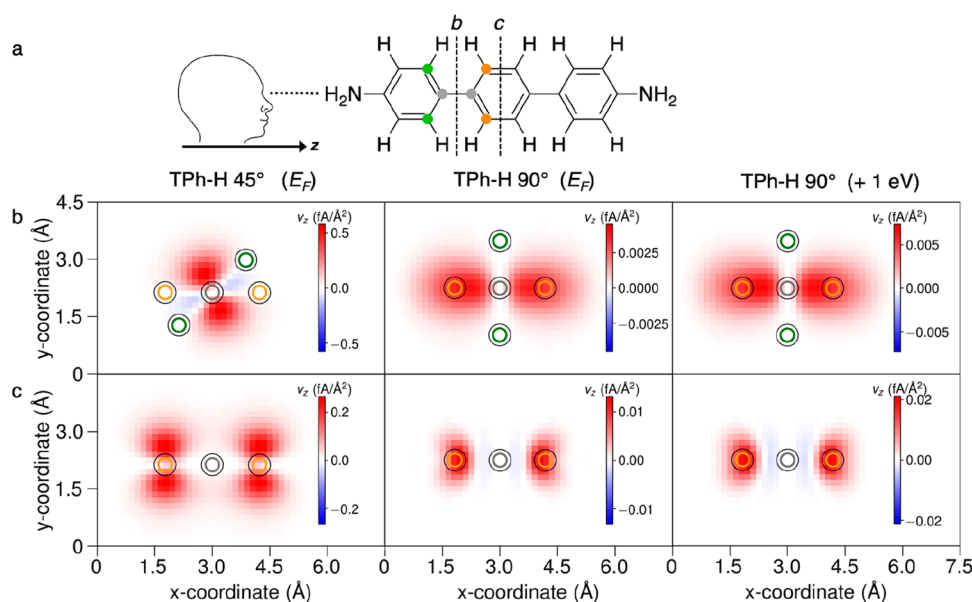

Figure 3. Ballistic current density through select surfaces of **TPh-H** at 45° and 90° axial torsion. Surfaces are chosen perpendicular to the transport direction, and the current density is therefore plotted as the z-component of the current density vector field. (a) Designation of the two surfaces perpendicular to the transport direction and color code of atoms shown in the current density plots. The atom designation is read looking from left to right. (b) Current density through surface b for **TPh-H** at 45° at the Fermi energy, 90° at the Fermi energy, and 90° at +1 eV. (c) Current density through surface c for **TPh-H** at 45° at the Fermi energy, 90° at the Fermi energy, and 90° at +1 eV.
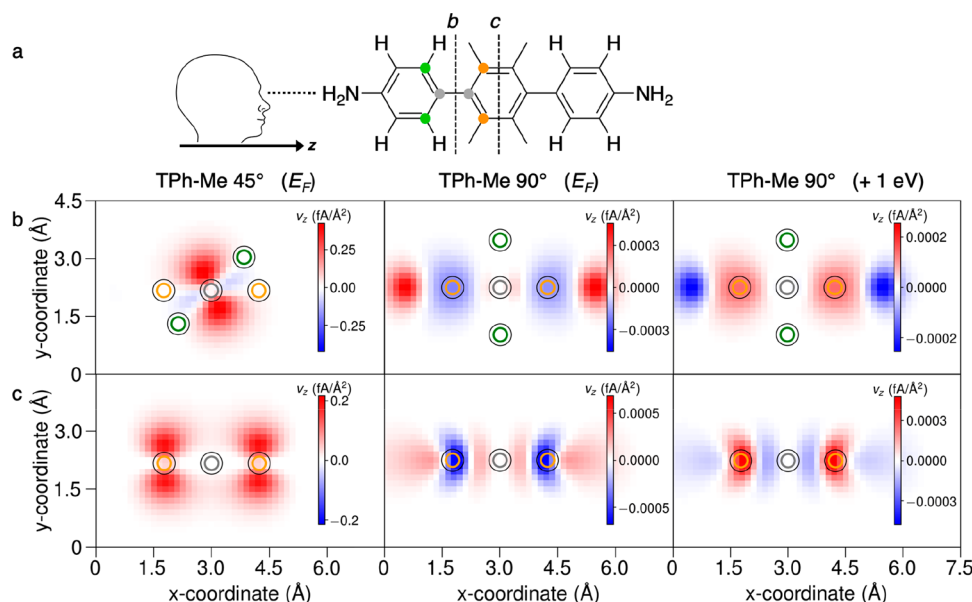
Figure 4. Ballistic current density through select surfaces of **TPh-Me** at 45° and 90° axial torsion. Surfaces are chosen perpendicular to the transport direction, and the current density is therefore plotted as the *z*-component of the current density vector field. (a) Designation of the two surfaces perpendicular to the transport direction and color code of atoms shown in the current density plots. The atom designation is read looking from left to right. (b) Current density through surface b for **TPh-Me** at 45° at the Fermi energy, 90° at the Fermi energy, and 90° at +1 eV. (c) Current density through surface c for **TPh-Me** at 45° at the Fermi energy, 90° at the Fermi energy, and 90° at +1 eV.

At 45° in Figures 3b and 4b, in both **TPh-H** and **TPh-Me**, there is clear forward current (red in the heat map) and two nodal planes, one for the π-system of each ring, thus indicating it is π−π interactions mediate the electronic coupling between the two rings. At 45° in Figures 3c and 4c both **TPh-H** and **TPh-Me** show clear current through the π-system of the central phenyl ring (current density above and below the plane of the ring with a nodal plane in the plane of the ring). As expected, the current is mediated by the π−system throughout these molecules.

At 90° the pattern of the current density is different. Considering first the pattern of the current density at the Fermi energy, in **TPh-H**, it is clear that the π-system of the outer ring(s) matches the symmetry of the σ-system of the central ring (Figure 3b). That is, the current is mediated by the π-system of the first ring (current density above and below the plane of the ring), the σ-system of the central ring (current density in the plane of the ring, Figure 3c), and again the π-system of the third ring. In **TPh-Me** at the Fermi energy, the current is quite different despite the structural similarity to **TPh-H**. There are strong backward currents (blue in the heat-map in both Figure 4b,c). We note here that destructive interference effects cannot be seen directly in the current density. The current density strictly only provides us with information about the (here small) current that continues to flow, rather than the current that has been suppressed due to interference. The evidence of destructive interference that can be found in the current density is ring currents that change direction.[68] Thus, while we see strong backward currents in the current density at the Fermi energy for **TPh-Me**, this is not in and of itself evidence of interference. Instead, we plot the current density at 1 eV above the Fermi energy, as it is clear from the transmission shown in Figure 2 that this energy is on the other side of the minimum transmission for both **TPh-Me** and **TPh-H**. The energy dependence of the current density is qualitatively different for the two systems. In **TPh-H** the

pattern of current density is essentially energy independent, whereas **TPh-Me** the forward and backward currents (red and blue regions) are reversed for 1 eV versus the Fermi energy. Beyond the qualitative differences in the transmission dips, sharp in the case of **TPh-Me** versus smooth for **TPh-H**, these differences in the energy dependence of the current density provides further evidence that the methyl substituents result in destructive σ-interference for these systems. Finally, we verify that it is the π-system that mediates the current in the first and last ring in all the triphenyl systems in Figure S4. Thus, it is the same π−σ−π interaction through the three rings that mediates the current in both **TPh-Me** and **TPh-H** at dihedral angles close to 90°. However, the methyl substituents effectively shut down the σ-transmission in the central ring due to destructive σ-interference. This is the cause of the large transmission difference of the two systems at 90° torsion that is seen in Figure 2.

As a final test of this comprehensive understanding of the conduction suppression in the triphenyl systems, we explore two similar systems where the central ring is partially saturated, thus providing an alternative approach to locally disrupting conjugation. Shown in Figure 5a, **Sat-H** has one double-bond less in the central ring as two hydrogens have been added to saturate two opposite carbon atoms; likewise, **Sat-Me** has two extra methyl groups on opposite carbon atoms in the central ring. In these systems there is no continuous π-system through the molecule, and the current will always be mediated to some extent by the σ-system of the central ring. Breaking the conjugation through the molecule in this way has the expected effect. In Figure 5b, the transmission of **Sat-H** is over an order of magnitude lower than **TPh-H** at dihedral angles below 45° due to the loss of a continuous π-system. But as the axial torsion of the two molecules approaches 90°, the transmission at the Fermi energy becomes very similar because transport through the π-system of the central ring is suppressed in both cases.
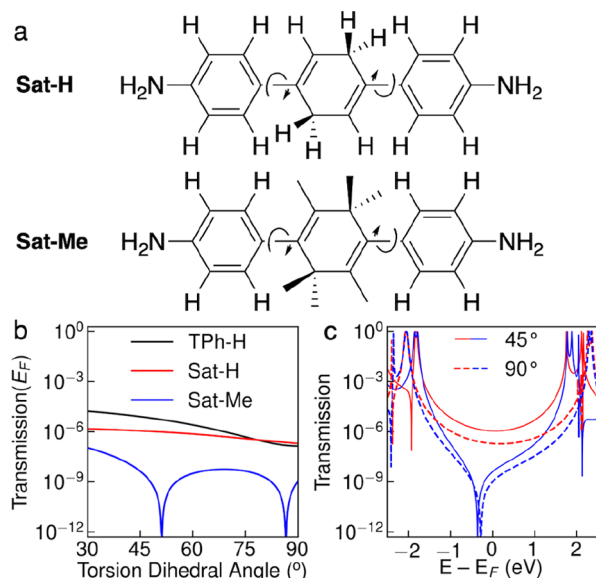
Figure 5. Transmission of triphenyl where two carbons have been saturated; i.e., the central ring is a cyclohexadiene. (a) Chemical structures of the partially saturated amine-functionalized triphenyl (**Sat-H**) and centrally methylated (**Sat-Me**) triphenyl. (b) Transmission of **Sat-H** (red) and **Sat-Me** (blue) at the Fermi energy as a function of dihedral angle. (c) Transmission as a function of energy for **Sat-H** (red) and **Sat-Me** (blue) calculated at 45° (full lines) and 90° (dashed lines) dihedral angles. The transmission of the optimized conformations are shown in Figure S9.

The transmission through **Sat-Me** is quite different. The transmission at the Fermi energy (Figure 5b) is suppressed over the full range of dihedral angles, even when the rings are near-planar. Looking at the full transmission plot in Figure 5c, it is clear that the antiresonance in the transmission is now almost independent of axial torsion. The transmission is always low for **Sat-Me** because the transmission is always mediated by the σ-system of the methylated central ring. The relatively small chemical difference of changing hydrogen to methyl substituents on the central ring, has a major effect on the electron transport properties because of the σ-interference effect.

In this and recent work our focus has been on the effect of methyl substituents, but of course other substituents may provide a similar effect. In Supporting Information part E, we have tested halide and phenyl substituted systems, which all show similar degrees of suppression as that in the methyl-substituted systems. Given that destructive quantum interference effects in both σ- and π-systems can be controlled with chemical design, we foresee that it will be possible to engineer highly insulating and polarizable molecules. Finally, we also note that our current density calculations of phenyl-substituted triphenyl, included in Supporting Information part F, show little indication of current through peripheral nonbonded paths due to through-space conjugation; recent experimental results may need to be reinterpreted.[69,70]

In summary, we have demonstrated that it is possible to simultaneously suppress π- and σ-transmission of biphenyl and triphenyl systems using destructive σ-interference and local disruption of conjugation. The interference effect is weak in hydrogen-substituted systems but can effectively suppress the σ-transmission in methyl-substituted phenyl rings, a substituent that also shifts minimum energy structures toward the

dihedral angles that support maximal suppression of the π-transport. Substituted oligophenyls are promising systems for further research in molecule-based dielectrics, as they indicate that it is indeed possible to realize conjugated insulators at the single-molecule level.

ASSOCIATED CONTENT

Ⓢ Supporting Information

The Supporting Information is available free of charge at https://pubs.acs.org/doi/10.1021/acs.jpclett.0c01727.

Junction structures in xyz format (ZIP)

Computational methods, biphenyl current density, ladder C model, triphenyl current density convergence, effect of substituted triphenyl, hexaphenyl current density, and transmission of optimized conformations (PDF)

AUTHOR INFORMATION

Corresponding Author

Gemma C. Solomon − *Nano-Science Center and Department of Chemistry, University of Copenhagen, DK-2100 Copenhagen Ø, Denmark;* Ⓞ orcid.org/0000-0002-2018-1529; Email: gsolomon@chem.ku.dk

Author

Marc H. Garner − *Nano-Science Center and Department of Chemistry, University of Copenhagen, DK-2100 Copenhagen Ø, Denmark;* Ⓞ orcid.org/0000-0002-7270-8353

Complete contact information is available at: https://pubs.acs.org/10.1021/acs.jpclett.0c01727

Notes

The authors declare no competing financial interest.

REFERENCES

(1) Kingon, A. I.; Maria, J.-P.; Streiffer, S. K. Alternative Dielectrics to Silicon Dioxide for Memory and Logic Devices. *Nature* **2000**, *406*, 1032−1038.

(2) Robertson, J.; Wallace, R. M. High-K Materials and Metal Gates for Cmos Applications. *Mater. Sci. Eng., R* **2015**, *88*, 1−41.

(3) Khan, H. N.; Hounshell, D. A.; Fuchs, E. R. H. Science and Research Policy at the End of Moore's Law. *Nature Electronics* **2018**, *1*, 14−21.

(4) Chen, R.; Li, Y.-C.; Cai, J.-M.; Cao, K.; Lee, H.-B.-R. Atomic Level Deposition to Extend Moore's Law and Beyond. *Int. J. Extrem. Manuf.* **2020**, *2*, 022002.

(5) Yoon, M.-H.; Facchetti, A.; Marks, T. J. σ-π Molecular Dielectric Multilayers for Low-Voltage Organic Thin-Film Transistors. *Proc. Natl. Acad. Sci. U. S. A.* **2005**, *102*, 4678.

(6) Ha, Y.-G.; Everaerts, K.; Hersam, M. C.; Marks, T. J. Hybrid Gate Dielectric Materials for Unconventional Electronic Circuitry. *Acc. Chem. Res.* **2014**, *47*, 1019−1028.

(7) Bergfield, J. P.; Heitzer, H. M.; Van Dyck, C.; Marks, T. J.; Ratner, M. A. Harnessing Quantum Interference in Molecular Dielectric Materials. *ACS Nano* **2015**, *9*, 6412−6418.

(8) Heitzer, H. M.; Marks, T. J.; Ratner, M. A. Computation of Dielectric Response in Molecular Solids for High Capacitance Organic Dielectrics. *Acc. Chem. Res.* **2016**, *49*, 1614−1623.

(9) Jones, L. O.; Mosquera, M. A.; Fu, B.; Schatz, G. C.; Marks, T. J.; Ratner, M. A. Quantum Interference and Substantial Property Tuning in Conjugated Z-Ortho-Regio-Resistive Organic (Zorro) Junctions. *Nano Lett.* **2019**, *19*, 8956−8963.

(10) Chen, H.; Zhang, W.; Li, M.; He, G.; Guo, X. Interface Engineering in Organic Field-Effect Transistors: Principles, Applications, and Perspectives. *Chem. Rev.* **2020**, *120*, 2879−2949.

(11) Xie, Z.; Bâldea, I.; Oram, S.; Smith, C. E.; Frisbie, C. D. Effect of Heteroatom Substitution on Transport in Alkanedithiol-Based Molecular Tunnel Junctions: Evidence for Universal Behavior. *ACS Nano* **2017**, *11*, 569−578.

(12) Li, H.; Garner, M. H.; Su, T. A.; Jensen, A.; Inkpen, M. S.; Steigerwald, M. L.; Venkataraman, L.; Solomon, G. C.; Nuckolls, C. Extreme Conductance Suppression in Molecular Siloxanes. *J. Am. Chem. Soc.* **2017**, *139*, 10212−10215.

(13) Metzger, R. M. Quo Vadis, Unimolecular Electronics? *Nanoscale* **2018**, *10*, 10316−10332.

(14) Garner, M. H.; Li, H.; Chen, Y.; Su, T. A.; Shangguan, Z.; Paley, D. W.; Liu, T.; Ng, F.; Li, H.; Xiao, S.; et al. Comprehensive Suppression of Single-Molecule Conductance Using Destructive σ-Interference. *Nature* **2018**, *558*, 415−419.

(15) Guédon, C. M.; Valkenier, H.; Markussen, T.; Thygesen, K. S.; Hummelen, J. C.; van der Molen, S. J. Observation of Quantum Interference in Molecular Charge Transport. *Nat. Nanotechnol.* **2012**, *7*, 305.

(16) Li, X.; Tan, Z.; Huang, X.; Bai, J.; Liu, J.; Hong, W. Experimental Investigation of Quantum Interference in Charge Transport through Molecular Architectures. *J. Mater. Chem. C* **2019**, *7*, 12790−12808.

(17) Herrmann, C. Electronic Communication as a Transferable Property of Molecular Bridges? *J. Phys. Chem. A* **2019**, *123*, 10205−10223.

(18) Sautet, P.; Joachim, C. Electronic Interference Produced by a Benzene Embedded in a Polyacetylene Chain. *Chem. Phys. Lett.* **1988**, *153*, 511−516.

(19) Cardamone, D. M.; Stafford, C. A.; Mazumdar, S. Controlling Quantum Transport through a Single Molecule. *Nano Lett.* **2006**, *6*, 2422−2426.

(20) Yoshizawa, K.; Tada, T.; Staykov, A. Orbital Views of the Electron Transport in Molecular Devices. *J. Am. Chem. Soc.* **2008**, *130*, 9406−9413.

(21) Solomon, G. C.; Andrews, D. Q.; Hansen, T.; Goldsmith, R. H.; Wasielewski, M. R.; Van Duyne, R. P.; Ratner, M. A. Understanding Quantum Interference in Coherent Molecular Conduction. *J. Chem. Phys.* **2008**, *129*, 054701.

(22) Markussen, T.; Stadler, R.; Thygesen, K. S. The Relation between Structure and Quantum Interference in Single Molecule Junctions. *Nano Lett.* **2010**, *10*, 4260−4265.

(23) Kiguchi, M.; Nakamura, H.; Takahashi, Y.; Takahashi, T.; Ohto, T. Effect of Anchoring Group Position on Formation and Conductance of a Single Disubstituted Benzene Molecule Bridging Au Electrodes: Change of Conductive Molecular Orbital and Electron Pathway. *J. Phys. Chem. C* **2010**, *114*, 22254−22261.

(24) Solomon, G. C.; Andrews, D. Q.; Goldsmith, R. H.; Hansen, T.; Wasielewski, M. R.; Van Duyne, R. P.; Ratner, M. A. Quantum Interference in Acyclic Systems: Conductance of Cross-Conjugated Molecules. *J. Am. Chem. Soc.* **2008**, *130*, 17301−17308.

(25) Ke, S.-H.; Yang, W.; Baranger, H. U. Quantum-Interference-Controlled Molecular Electronics. *Nano Lett.* **2008**, *8*, 3257−3261.

(26) Solomon, G. C.; Andrews, D. Q.; Van Duyne, R. P.; Ratner, M. A. Electron Transport through Conjugated Molecules: When the π System Only Tells Part of the Story. *ChemPhysChem* **2009**, *10*, 257−264.

(27) Borges, A.; Fung, E. D.; Ng, F.; Venkataraman, L.; Solomon, G. C. Probing the Conductance of the σ-System of Bipyridine Using Destructive Interference. *J. Phys. Chem. Lett.* **2016**, *7*, 4825−4829.

(28) Mayor, M.; Weber, H. B.; Reichert, J.; Elbing, M.; von Hänisch, C.; Beckmann, D.; Fischer, M. Electric Current through a Molecular

Rod—Relevance of the Position of the Anchor Groups. *Angew. Chem., Int. Ed.* **2003**, *42*, 5834−5838.

(29) Taniguchi, M.; Tsutsui, M.; Mogi, R.; Sugawara, T.; Tsuji, Y.; Yoshizawa, K.; Kawai, T. Dependence of Single-Molecule Conductance on Molecule Junction Symmetry. *J. Am. Chem. Soc.* **2011**, *133*, 11426−11429.

(30) Aradhya, S. V.; Meisner, J. S.; Krikorian, M.; Ahn, S.; Parameswaran, R.; Steigerwald, M. L.; Nuckolls, C.; Venkataraman, L. Dissecting Contact Mechanics from Quantum Interference in Single-Molecule Junctions of Stilbene Derivatives. *Nano Lett.* **2012**, *12*, 1643−1647.

(31) Arroyo, C. R.; Tarkuc, S.; Frisenda, R.; Seldenthuis, J. S.; Woerde, C. H. M.; Eelkema, R.; Grozema, F. C.; van der Zant, H. S. J. Signatures of Quantum Interference Effects on Charge Transport through a Single Benzene Ring. *Angew. Chem., Int. Ed.* **2013**, *52*, 3152−3155.

(32) Arroyo, C. R.; Frisenda, R.; Moth-Poulsen, K.; Seldenthuis, J. S.; Bjørnholm, T.; van der Zant, H. S. J. Quantum Interference Effects at Room Temperature in Opv-Based Single-Molecule Junctions. *Nanoscale Res. Lett.* **2013**, *8*, 234.

(33) Liu, X.; Sangtarash, S.; Reber, D.; Zhang, D.; Sadeghi, H.; Shi, J.; Xiao, Z.-Y.; Hong, W.; Lambert, C. J.; Liu, S.-X. Gating of Quantum Interference in Molecular Junctions by Heteroatom Substitution. *Angew. Chem., Int. Ed.* **2017**, *56*, 173−176.

(34) Huang, B.; Liu, X.; Yuan, Y.; Hong, Z.-W.; Zheng, J.-F.; Pei, L.-Q.; Shao, Y.; Li, J.-F.; Zhou, X.-S.; Chen, J.-Z.; et al. Controlling and Observing Sharp-Valleyed Quantum Interference Effect in Single Molecular Junctions. *J. Am. Chem. Soc.* **2018**, *140*, 17685−17690.

(35) Li, Y.; Buerkle, M.; Li, G.; Rostamian, A.; Wang, H.; Wang, Z.; Bowler, D. R.; Miyazaki, T.; Xiang, L.; Asai, Y.; et al. Gate Controlling of Quantum Interference and Direct Observation of Anti-Resonances in Single Molecule Charge Transport. *Nat. Mater.* **2019**, *18*, 357−363.

(36) Jiang, F.; Trupp, D. I.; Algethami, N.; Zheng, H.; He, W.; Alqorashi, A.; Zhu, C.; Tang, C.; Li, R.; Liu, J.; et al. Turning the Tap: Conformational Control of Quantum Interference to Modulate Single-Molecule Conductance. *Angew. Chem., Int. Ed.* **2019**, *58*, 18987−18993.

(37) Li, S.; Yu, H.; Schwieter, K.; Chen, K.; Li, B.; Liu, Y.; Moore, J. S.; Schroeder, C. M. Charge Transport and Quantum Interference Effects in Oxazole-Terminated Conjugated Oligomers. *J. Am. Chem. Soc.* **2019**, *141*, 16079−16084.

(38) Manrique, D. Z.; Huang, C.; Baghernejad, M.; Zhao, X.; Al-Owaedi, O. A.; Sadeghi, H.; Kaliginedi, V.; Hong, W.; Gulcur, M.; Wandlowski, T.; et al. A Quantum Circuit Rule for Interference Effects in Single-Molecule Electrical Junctions. *Nat. Commun.* **2015**, *6*, 6389.

(39) George, C. B.; Ratner, M. A.; Lambert, J. B. Strong Conductance Variation in Conformationally Constrained Oligosilane Tunnel Junctions. *J. Phys. Chem. A* **2009**, *113*, 3876−3880.

(40) Li, H.; Garner, M. H.; Shangguan, Z.; Chen, Y.; Zheng, Q.; Su, T. A.; Neupane, M.; Liu, T.; Steigerwald, M. L.; Ng, F.; et al. Large Variations in the Single-Molecule Conductance of Cyclic and Bicyclic Silanes. *J. Am. Chem. Soc.* **2018**, *140*, 15080−15088.

(41) Garner, M. H.; Li, H.; Neupane, M.; Zou, Q.; Liu, T.; Su, T. A.; Shangguan, Z.; Paley, D. W.; Ng, F.; Xiao, S.; et al. Permethylation Introduces Destructive Quantum Interference in Saturated Silanes. *J. Am. Chem. Soc.* **2019**, *141*, 15471−15476.

(42) Li, C.; Pobelov, I.; Wandlowski, T.; Bagrets, A.; Arnold, A.; Evers, F. Charge Transport in Single Au | Alkanedithiol | Au Junctions: Coordination Geometries and Conformational Degrees of Freedom. *J. Am. Chem. Soc.* **2008**, *130*, 318−326.

(43) Paulsson, M.; Krag, C.; Frederiksen, T.; Brandbyge, M. Conductance of Alkanedithiol Single-Molecule Junctions: A Molecular Dynamics Study. *Nano Lett.* **2009**, *9*, 117−121.

(44) Paz, S. A.; Zoloff Michoff, M. E.; Negre, C. F. A.; Olmos-Asar, J. A.; Mariscal, M. M.; Sánchez, C. G.; Leiva, E. P. M. Configurational Behavior and Conductance of Alkanedithiol Molecular Wires from Accelerated Dynamics Simulations. *J. Chem. Theory Comput.* **2012**, *8*, 4539−4545.

(45) Mejía, L.; Renaud, N.; Franco, I. Signatures of Conformational Dynamics and Electrode-Molecule Interactions in the Conductance Profile During Pulling of Single-Molecule Junctions. *J. Phys. Chem. Lett.* **2018**, *9*, 745−750.

(46) Woitellier, S.; Launay, J. P.; Joachim, C. The Possibility of Molecular Switching: Theoretical Study of [(Nh$_3$)$_5$Ru-4,4'-Bipy-Ru(Nh$_3$)$_5$]$^{5+}$. *Chem. Phys.* **1989**, *131*, 481−488.

(47) Venkataraman, L.; Klare, J. E.; Nuckolls, C.; Hybertsen, M. S.; Steigerwald, M. L. Dependence of Single-Molecule Junction Conductance on Molecular Conformation. *Nature* **2006**, *442*, 904−907.

(48) Vonlanthen, D.; Mishchenko, A.; Elbing, M.; Neuburger, M.; Wandlowski, T.; Mayor, M. Chemically Controlled Conductivity: Torsion-Angle Dependence in a Single-Molecule Biphenyldithiol Junction. *Angew. Chem., Int. Ed.* **2009**, *48*, 8886−8890.

(49) Mishchenko, A.; Vonlanthen, D.; Meded, V.; Bürkle, M.; Li, C.; Pobelov, I. V.; Bagrets, A.; Viljas, J. K.; Pauly, F.; Evers, F.; et al. Influence of Conformation on Conductance of Biphenyl-Dithiol Single-Molecule Contacts. *Nano Lett.* **2010**, *10*, 156−163.

(50) Mishchenko, A.; Zotti, L. A.; Vonlanthen, D.; Bürkle, M.; Pauly, F.; Cuevas, J. C.; Mayor, M.; Wandlowski, T. Single-Molecule Junctions Based on Nitrile-Terminated Biphenyls: A Promising New Anchoring Group. *J. Am. Chem. Soc.* **2011**, *133*, 184−187.

(51) Lörtscher, E.; Elbing, M.; Tschudy, M.; von Hänisch, C.; Weber, H. B.; Mayor, M.; Riel, H. Charge Transport through Molecular Rods with Reduced π-Conjugation. *ChemPhysChem* **2008**, *9*, 2252−2258.

(52) Grunder, S.; Stoddart, J. F. Giving Substance to the Losanitsch Series. *Chem. Commun.* **2012**, *48*, 3158−3160.

(53) Bi, H.; Palma, C.-A.; Gong, Y.; Hasch, P.; Elbing, M.; Mayor, M.; Reichert, J.; Barth, J. V. Voltage-Driven Conformational Switching with Distinct Raman Signature in a Single-Molecule Junction. *J. Am. Chem. Soc.* **2018**, *140*, 4835−4840.

(54) Chen, Z.; Chen, L.; Liu, J.; Li, R.; Tang, C.; Hua, Y.; Chen, L.; Shi, J.; Yang, Y.; Liu, J.; et al. Modularized Tuning of Charge Transport through Highly Twisted and Localized Single-Molecule Junctions. *J. Phys. Chem. Lett.* **2019**, *10*, 3453−3458.

(55) Shultz, D. A.; Kirk, M. L.; Zhang, J.; Stasiw, D. E.; Wang, G.; Yang, J.; Habel-Rodriguez, D.; Stein, B. W.; Sommer, R. D. Spectroscopic Signatures of Resonance Inhibition Reveal Differences in Donor−Bridge and Bridge−Acceptor Couplings. *J. Am. Chem. Soc.* **2020**, *142*, 4916−4924.

(56) Bürkle, M.; Viljas, J. K.; Vonlanthen, D.; Mishchenko, A.; Schön, G.; Mayor, M.; Wandlowski, T.; Pauly, F. Conduction Mechanisms in Biphenyl Dithiol Single-Molecule Junctions. *Phys. Rev. B: Condens. Matter Mater. Phys.* **2012**, *85*, 075417.

(57) Kang, H.; Facchetti, A.; Zhu, P.; Jiang, H.; Yang, Y.; Cariati, E.; Righetto, S.; Ugo, R.; Zuccaccia, C.; Macchioni, A.; et al. Exceptional Molecular Hyperpolarizabilities in Twisted π-Electron System Chromophores. *Angew. Chem., Int. Ed.* **2005**, *44*, 7922−7925.

(58) Shi, Y.; Frattarelli, D.; Watanabe, N.; Facchetti, A.; Cariati, E.; Righetto, S.; Tordin, E.; Zuccaccia, C.; Macchioni, A.; Wegener, S. L.; et al. Ultra-High-Response, Multiply Twisted Electro-Optic Chromophores: Influence of π-System Elongation and Interplanar Torsion on Hyperpolarizability. *J. Am. Chem. Soc.* **2015**, *137*, 12521−12538.

(59) Lou, A. J. T.; Marks, T. J. A Twist on Nonlinear Optics: Understanding the Unique Response of π-Twisted Chromophores. *Acc. Chem. Res.* **2019**, *52*, 1428−1438.

(60) Larsen, A. H.; Mortensen, J. J.; Blomqvist, J.; Castelli, I. E.; Christensen, R.; Dułak, M.; Friis, J.; Groves, M. N.; Hammer, B.; Hargus, C.; et al. The Atomic Simulation Environment—a Python Library for Working with Atoms. *J. Phys.: Condens. Matter* **2017**, *29*, 273002.

(61) Enkovaara, J.; Rostgaard, C.; Mortensen, J. J.; Chen, J.; Dułak, M.; Ferrighi, L.; Gavnholt, J.; Glinsvad, C.; Haikola, V.; Hansen, H. A.; et al. Electronic Structure Calculations with Gpaw: A Real-Space Implementation of the Projector Augmented-Wave Method. *J. Phys.: Condens. Matter* **2010**, *22*, 253202.

(62) Garner, M. H.; Koerstz, M.; Jensen, J. H.; Solomon, G. C. The Bicyclo[2.2.2]Octane Motif: A Class of Saturated Group 14 Quantum Interference Based Single-Molecule Insulators. *J. Phys. Chem. Lett.* **2018**, *9*, 6941−6947.

(63) Jensen, A.; Garner, M. H.; Solomon, G. C. When Current Does Not Follow Bonds: Current Density in Saturated Molecules. *J. Phys. Chem. C* **2019**, *123*, 12042−12051.

(64) Perdew, J. P.; Burke, K.; Ernzerhof, M. Generalized Gradient Approximation Made Simple. *Phys. Rev. Lett.* **1996**, *77*, 3865−3868.

(65) Frisch, M. J.; Trucks, G. W.; Schlegel, H. B.; Scuseria, G. E.; Robb, M. A.; Cheeseman, J. R.; Scalmani, G.; Barone, V.; Mennucci, B.; Petersson, G. A.; et al. *Gaussian 09*, Rev. D.01; Gaussian, Inc.: Wallingford, CT, 2013.

(66) Schepers, T.; Michl, J. Optimized Ladder C and Ladder H Models for Sigma Conjugation: Chain Segmentation in Polysilanes. *J. Phys. Org. Chem.* **2002**, *15*, 490−498.

(67) Jovanovic, M.; Michl, J. Effect of Conformation on Electron Localization and Delocalization in Infinite Helical Chains [X(Ch$_3$)$_2$]$_\infty$ (X = Si, Ge, Sn, and Pb). *J. Am. Chem. Soc.* **2019**, *141*, 13101−13113.

(68) Solomon, G. C.; Herrmann, C.; Hansen, T.; Mujica, V.; Ratner, M. A. Exploring Local Currents in Molecular Junctions. *Nat. Chem.* **2010**, *2*, 223.

(69) Zhen, S.; Mao, J.-C.; Chen, L.; Ding, S.; Luo, W.; Zhou, X.-S.; Qin, A.; Zhao, Z.; Tang, B. Z. Remarkable Multichannel Conductance of Novel Single-Molecule Wires Built on through-Space Conjugated Hexaphenylbenzene. *Nano Lett.* **2018**, *18*, 4200−4205.

(70) Li, Y.; Xiao, B.; Chen, R.; Chen, H.; Dong, J.; Liu, Y.; Chang, S. Single-Molecule Conductance Investigation of Bdt Derivatives: An Additional Pattern Found to Induce through-Space Channels Beyond π−π Stacking. *Chem. Commun.* **2019**, *55*, 8325−8328.